Open Access

Journal of Energy and Power Technology

LIDSEN Publishing Inc.

Original Research

Analysis of LoRa Transmission Delay on Dynamic Performance of Standalone DC Microgrids

Cherechi Ndukwe [1, †, *], M. Tariq Iqbal [1, †], Jahangir Khan [2, †], Mohsin Jamil [1, †]

1. Faculty of Engineering and Applied Sciences, Memorial University of Newfoundland, St John's, Canada; E-Mails: cindukwe@mun.ca; tariq@mun.ca; mjamil@mun.ca
2. Transmission Engineering BC Hydro, Burnaby, British Columbia, Canada; E-Mail: mjakhan@ieee.org

† These authors contributed equally to this work.

* **Correspondence:** Cherechi Ndukwe; E-Mail: cindukwe@mun.ca

Academic Editor: Zhao Yang Dong

Special Issue: Planning, Control and Operation of Hybrid Power Systems

Journal of Energy and Power Technology
2022, volume 4, issue 2
doi:10.21926/jept.2202022

Received: April 18, 2022
Accepted: June 19, 2022
Published: June 26, 2022

Abstract

One important aspect toward proper and stable functioning of a communication-based controlled microgrid is data transmission. Consequently, an analysis of the effect of data transmission delay is of significance for any chosen communication protocol. This paper focuses on the effect of employing LoRa for data transfer at the secondary control level of a standalone DC microgrid. It analyses the effect of LoRa transmission delay on the dynamic performance of DC microgrids. This paper simulates a community DC microgrid that operates in three modes: PV mode, battery mode and generator mode. This microgrid operates as a centralized communication-based controlled microgrid, with the secondary control level operating as an event-driven level. The system incorporates a hierarchical system where data is transferred between the various distributed energy resources (DERs) local controllers and the microgrid central controller (MGCC). Simulations for three scenarios are presented. In the first scenario, the microgrid is designed and simulated without a communication delay to

observe the system behavior. Then LoRa transmission delay is calculated for the various signals transferred between the MGCC and the local controllers. This delay is introduced into the simulation as transport delays and the system exhibits a level of stability degradation. Subsequently, a time delay compensation system is incorporated into the system for more robust operation. The delay compensation is applied in two simulation scenarios. In the first scenario, the system inductor (L) and capacitor (C) components are re-calculated, and the system is re-simulated to get a stable system even with the applied communication delay. In the second scenario, the proportional integrator (PI) controller in the microgrid central controller is re-designed to a more robust form to compensate for the delay caused by the LoRa transmission. The results obtained from the two modified simulations realize a stable DC microgrid. This system modification allows for system stability again, similar to the simulation when the microgrid operated without any communication delay. This, therefore, demonstrates that with proper system design and implementation, low bandwidth communication systems such as LoRa can be effectively employed for data transfer in event-driven communication-based controlled DC microgrids.

Keywords
DC microgrid; microgrid control; LoRa communication; data transmission delay

1. Introduction

Microgrids are important elements towards full realization of smart grids, which are already in existence in most developed countries. Such systems have the potential to attain higher grid resilience [1, 2]. The United States Department of Energy has defined microgrid as an interconnection of distributed energy resources (DERs), energy storage systems (ESS) and groups of interconnected loads. Microgrids have been developed to either operate in grid-connected mode or in standalone (islanded) mode [3, 4]. The grid-connected microgrid is tied to a larger network and supported by the microgrid DERs in times of faults, blackouts etc. On the other hand, when the microgrid is directly supplying the loads with power generated by the DERs, it is referred to as islanded mode of operation.

Presently, microgrids are mainly classified as AC, DC, or hybrid AC/DC microgrids. This classification is mainly focused on the common voltage of the microgrid [5]. DC microgrids have shown to be more efficient due to the lower amount of internal conversion required for power transfer to the loads [5]. This is the reason, most of the DERs and ESSs are DC systems [5]. The main known challenges to date are around the design of efficient protection systems [6-8]. As such, the hybrid system has been developed with consideration of the advantages of both AC and DC systems. Note that in this research paper, only DC microgrid is considered.

DC microgrids can be operated in two primary control modes: (1) voltage-droop control and (2) communication-based control. In voltage-droop control, system stability is achieved by the application of a virtual resistor to the converter's voltage regulator [5]. This enables current/power-sharing. The main advantage of this control method is its total reliance on system parameters, and as such it does not require any communication system for data transfer [9, 10]. However, the droop

control faces some challenges, which includes slow dynamic response and system voltage inaccuracies caused by circulation currents between the converters [11, 12]. This generally has a degrading effect on microgrid stability.

Communication-based control is based on continuous communication of various microgrid components for data transfer that facilitate control. Microgrids that are controlled using this method can be classified into centralized or decentralized systems [5]. In the centralized system, the main controller communicates with the local controllers of all components, which then sets various points and control actions based on the data obtained from the various controllers. On the other hand, a distributed system has no need for a central controller. As a result, it is immune to one of the main problems faced by the centralized system - a single point of failure. Understandably, the distributed control system is generally rather complex.

In recent times, research has focused on the employment of low bandwidth communication systems for data transfer within microgrids [13, 14]. From literature, it has been observed that the benefit of such systems is in reduced number of parameters to be transferred. Even though various schemes are being investigated to date, these analyses are done on a general level.

LoRa has been proposed and successfully implemented in a wide variety of applications in various fields of engineering and technology. With more focus on microgrids, this has also been proposed for data transfer at the secondary control level [14].

From various research and to the best of authors knowledge, there has not been any specific work that covers the effect of LoRa transmission delay on the dynamic performance of a DC microgrid. As such, this research brings novelty to the knowledge base.

This paper presents an analysis of LoRa for data transfer in a centralized communication-based controlled DC microgrid and focuses on the effects of LoRa transmission delay on the dynamic performance of a standalone system.

The main contributions of this paper include:

1) Design and simulation of a DC microgrid with LoRa transmission delay to observe the effect of the LoRa transmission delay on the microgrid dynamic performance.
2) Demonstration of a stable DC microgrid with LoRa as the data transfer system by proper component selection and system redesign.

This paper is organized as follows: Section 2 presents a description of the communication-based DC microgrid; Section 3 describes the mathematical characterization of LoRa data transmission delay; Section 4 describes the DC microgrid being studied; Section 5 presents the simulation results; Section 6 discusses the results. Key conclusions and recommendations for future work are presented in Section 7.

2. Communication-Based DC Microgrid Control

Communication-based DC microgrid control can be defined as a microgrid control technique that depends substantially on constant communication between various microgrid components for real-time update of system parameters and control commands. This technique is either centralized or fully distributed. In centralized communication-based control, all sensor (i.e., field devices) data are measured and transmitted from various controllers to the microgrid central controller (MGCC). The received parameters are processed, and if parameter discrepancies exist, the central controller sends back control commands and operation set points to maintain system stability [5]. In most

cases, this technique offers near optimal microgrid performance because the central microgrid controller constantly has real-time information of the microgrid resources. On the other hand, due to the total reliance of the microgrid reliability on the communication system, the system is susceptible to the single point of failure. This, therefore, emphasizes the importance of the reliable communication system for data transfer within microgrids employing this control technique.

In distributed communication-based control, the need for a central controller is not pressing as the local controllers have direct communication towards coordination and negotiation to achieve microgrid optimum stability [15]. This in turn, has an impact on system reliability. Furthermore, due to the distributed nature of this technique for microgrid control, it is immune to the single point of failure as with the centralized communication technique. However, system complexity of this technique has been the main limitation [16]. The centralized and distributed techniques are shown in Figure 1. In this research, a centralized communication-based microgrid control technique is employed for simplicity.

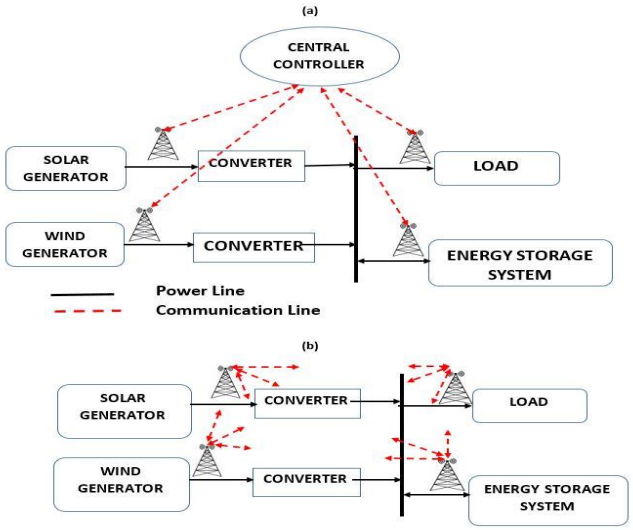

Figure 1 (a) Centralized communication microgrid control (b) distributed communication microgrid control.

Data and control commands transfer within microgrids can be either "state-driven" or "event-driven". State driven control is specifically based on continuous transfer of system state variables to the controller. These variables are constantly sampled and periodically transmitted. In the event-driven control, the controllers are only triggered by anomalies in the system. Hence, reducing the frequency of parameter transfer. Rather events trigger actions for system operation mode switch. This control, therefore, can function more with a low communication bandwidth than the state-driven control. The event-driven control presents some advantages such as low communication bandwidth requirements low computational process, which in turn saves energy [17, 18]. However, it is important to note that event-driven control requires a deep understanding of the system to increase system alertness thereby avoiding unexpected system events that might level to the system instability. State-driven control still dominates for microgrid control due to its already-existing experience and the possible difficulties involved in the development of event-driven control algorithm [17]. For State driven control, system performance has been the focus, while event-driven control may be suitable for certain applications to balance between control performance and

system efficiency. In microgrid control, as stated in [5], state-driven control is well employed in primary control between the sensors and the local controller sharing parameters such as gate pulses to the converters and electrical parameters. Furthermore, event driven control can be applied to secondary control levels where parameters such as event report, state changes, parameter reduction and command signals are transferred between the local controller and the central controller.

2.1 Microgrid Event-Driven Control

A hierarchical microgrid control structure is employed in this research. The primary control layer is consisted of local controllers that communicate continuously with various sensors connected to the DERs. This control level functions in the state-driven mode. The local controllers continuously monitor and measure the state variables that are vital to maintain various modes and operating points. In the secondary control layer, the microgrid central controller communicates with the local controllers and assigns operating modes for stability with reference to the changed parameters it received from the local controllers. The secondary control layer is event-controlled. The secondary control layer being event-controlled entails that it does not require continuous communication between the microgrid central controller, and the local controllers located at the various distributed generation (DG) units. This reduces the overall communication bandwidth requirements for data and command transfer.

The analysis in this paper strictly focuses on the dynamic performance of the secondary control level. Authors in [19] state that, in comparison, if the sampling frequency of a high bandwidth communication is f_s, then the low bandwidth communication protocol will have a sampling frequency of $\frac{f_s}{N}$ (meaning, there is a reduction of data amount to $\frac{1}{N}$ in low bandwidth communication), where N is the number of control periods. This analogy allows for the employment of low-bandwidth communication systems for event-driven secondary level control data transfer.

In event-driven control, during normal operations, communication only happens with an event that also results to a control action. Therefore, if the total sampling time during the control process $T_S = \sum_0^{N_S} T_{NS}$ [17], where N_s is the number of samples sent through the communication network during the control process and T_{NS} is the sampling time of one sample of N_s. Assuming the same sample duration, high bandwidth communication T_S will be higher than low bandwidth communication T_S. In event driven control, $T_S|_e = \sum_0^{m-1} T_{NS}$, where m is the number of events triggered during the control process.

Considering that events do not occur frequently, the $T_S|_e$ is very much lower compared to T_S in high and low bandwidth communication. This work employs an event-driven communication-based secondary level microgrid control.

3. LoRa Data Transmission Delay Mathematical Characterization

LoRa has recently been developed as a physical layer communication technique known very well for its low power consumption and long-range data transfer capabilities. These features have facilitated its significant growth for industrial applications for which microgrids is not an exception. Due to the proprietary nature of this communication protocol, there has not been a detailed mathematical description of the system. This section focuses on mathematical characterization of

LoRa transmission delay. LoRa is defined as a linear chirp signal because it corresponds to a waveform whose frequency increases or decreases linearly with time [20].

The following notations are used in the characterization, as shown in Table 1.

Table 1 LoRa Modulation Notations.

Notation	Description
f_c	Starting frequency of up-chirp
B_W	Bandwidth
SF	Spread factor used for modulation (usually, 7 to 12 in LoRa)
T	Data transfer period of chirp = $\frac{2^{SF}}{B_W}$
μ	+1 (up chirp) -1 (down chirp)
$\theta(t)$	Phase of the chirp signal
$c(t)$	Carrier signal
s(t)	Transmitted symbol waveform
$f(t)$	Instantaneous frequency of chirp signal

In LoRa modulation, the carrier signal, *c(t)*, is a linear up-chirp given by the expression:

$$c(t) = f(x) = \begin{cases} \exp(j\theta(t)), & 0 \le t \le T \\ 0, & o.w. \end{cases} \quad (1)$$

The instantaneous accumulated phase of the chirp signal $\theta(t)$ and the instantaneous frequency as a function of time are given by:

$$\theta(t) = 2\pi f_c + \pi\mu \frac{B_W}{T} t^2, \qquad 0 \le t \le T \quad (2)$$

$$f(t) = \frac{1}{2\pi}\frac{d\theta(t)}{dt} = f_c + \mu\frac{B_w}{T}t, \qquad 0 \le t \le T \quad (3)$$

Therefore, for a general case for symbol transmission, the transmitted symbol waveform s(t), is given by,

$$s(t) = \begin{cases} \exp(j\emptyset(t)), & 0 \le t \le T \\ 0, & o.w. \end{cases} \quad (4)$$

The instantaneous chirp frequency of the coded symbol is then defined as:

$$f(t) = \begin{cases} f_c + \mu\frac{B_W}{T}\left(t - \frac{K}{B_W}\right) + B_W, & 0 \le t \le \frac{K}{B_W} \\ f_c + \mu\frac{B_W}{T}\left(t - \frac{K}{B_W}\right), & \frac{K}{B_W} \le t \le T \end{cases} \quad (5)$$

Furthermore, the instantaneous accumulated phase of the coded symbol is then defined as:

$$\emptyset(t) = \begin{cases} 2\pi f_c t + 2\pi\mu \frac{B_w}{T}\left(\frac{t^2}{2} - \frac{K}{B_W}t\right) + 2\pi B_W t, & 0 \le t \le \frac{K}{B_W} \\ 2\pi f_c t + 2\pi\mu \frac{B_w}{T}\left(\frac{t^2}{2} - \frac{K}{B_W}t\right), & \frac{K}{B_W} \le t \le T \end{cases} \quad (6)$$

Traditionally, data is transmitted on LoRa communication technology as data packets in $BASE_{64}$ format. A detailed analysis of LoRa in the context of microgrid data transfer has been presented in [14] where the conversion is achieved in the following key steps:

a. Data preparation into ASCII text format.
b. Each letter of the ASCII text format is converted to ASCII binary format.
c. The binary codes obtained from the step above with 8 bits are joined together
d. The joined binary data is now split into 6-bit binary codes.
e. Each 6-bits is then converted to decimal value
f. Each decimal value is matched with a Base64 symbol on the Base64 table, where each decimal value from 0-63 has a matching symbol.

To further illustrate the LoRa transfer format, the above-stated steps are shown in Figure 2 for a measured 360 V (possible microgrid bus voltage).

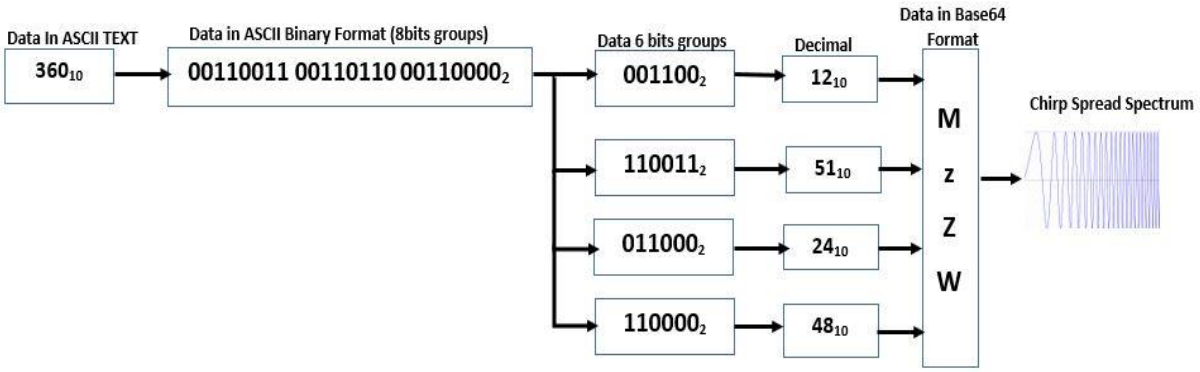

Figure 2 Representation of LoRa data formatting before transmission.

The structure of a basic LoRa data frame is shown in Figure 3.

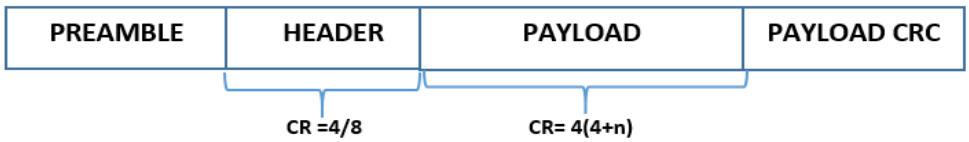

Figure 3 Structure of a LoRa frame.

The time to transfer each chip by a LoRa device depends on the bandwidth. This time is calculated as:

$$T_{chip} = \frac{1}{Bandwidth} \quad (7)$$

In LoRa communication, there are three statutory bandwidths through which data can be transmitted. These are: 125 kHz, 250 kHz, and 500 kHz [20]. The bandwidth can also be defined as the chip rate, which is the number of vibrations or wave cycles per second. Hence,

$$BW = R_C = Chip\ Rate \tag{8}$$

For a bandwidth of 125 KHz, the chip rate is 125000 chips/sec. Therefore,

$$T_{chip} = \frac{1}{125{,}000} = 0.000008\ sec$$

T_{chip} for the 125 kHz, 250 kHz and 500 kHz are 8µs, 4µs and 2µs respectively. This shows that with increased bandwidth there is a reduction in transmission time. The transmission time for a LoRa symbol T_{symbol} is calculated as:

$$T_{symbol} = \frac{2^{SF}}{BW} \tag{9}$$

where, SF is the spreading factor, and BW is the bandwidth.

From Equation (9), the time to transfer a symbol with the existing spreading factors (7-12) and the bandwidths are shown in Table 2.

Table 2 A comparison of LoRa transfer bandwidths delays.

SF	T_{symbol} (µs) @ BW = 125 KHz	T_{symbol} (µs) @ BW = 250 KHz	T_{symbol} (µs) @ BW = 500 KHz
7	1,024	512	256
8	2,048	1,024	512
9	4,096	2,048	1024
10	8,192	4,096	2048
11	16,384	8,192	4096
12	32,768	16,384	8,192

Table 2 shows that an increase in bandwidth has a decreasing effect on the data transmission time. Furthermore, an increase in the spreading factor increases the transmission time. The transmission time doubles with a one-step increase in the spreading factor (SF).

The expressions for calculating the data transmission time for a LoRa frame is given by:

$$T_{frame} = T_{preamble} + T_{payload} \tag{10}$$

$$T_{payload} = n_{payload} + T_{symbol} \tag{11}$$

$$n_{payload} = 8 + \max\left(ceil\left[\frac{8PL - 4SF + 28 + 16CRC - 20IH}{4(SF - 2DE)}\right](CR + 4), 0\right) \tag{12}$$

$$T_{preamble} = \left(n_{preamble} + 4.25\right)T_{symbol} \tag{13}$$

normally, $n_{preamble}$ = 8 for LoRa. Where, PL = number of bytes; IH = Implicit header (If Header is enabled, IH = 0 if Header is disabled, IH = 1); DE = low data optimization (DE = 1, enabled, 0 = disabled); CR = Coding rate (default = 1); CRC = 1 if enabled, 0 if disabled (default is 1).

4. Microgrid Case Study

The DC microgrid under study in this paper is shown in Figure 4. It is a community standalone DC microgrid that consists of a 1000 kW photovoltaic (PV) system connected to the DC bus through a DC/DC boost converter, a battery system integrated into the DC bus through a bidirectional DC/DC charger, a 630-kW diesel generator connected to the DC bus through a full-bridge rectifier. The microgrid bus voltage is 360 V DC, and the total DC community load of 300 kW. The values of the converter parameters as calculated for this simulation are shown in Table 3.

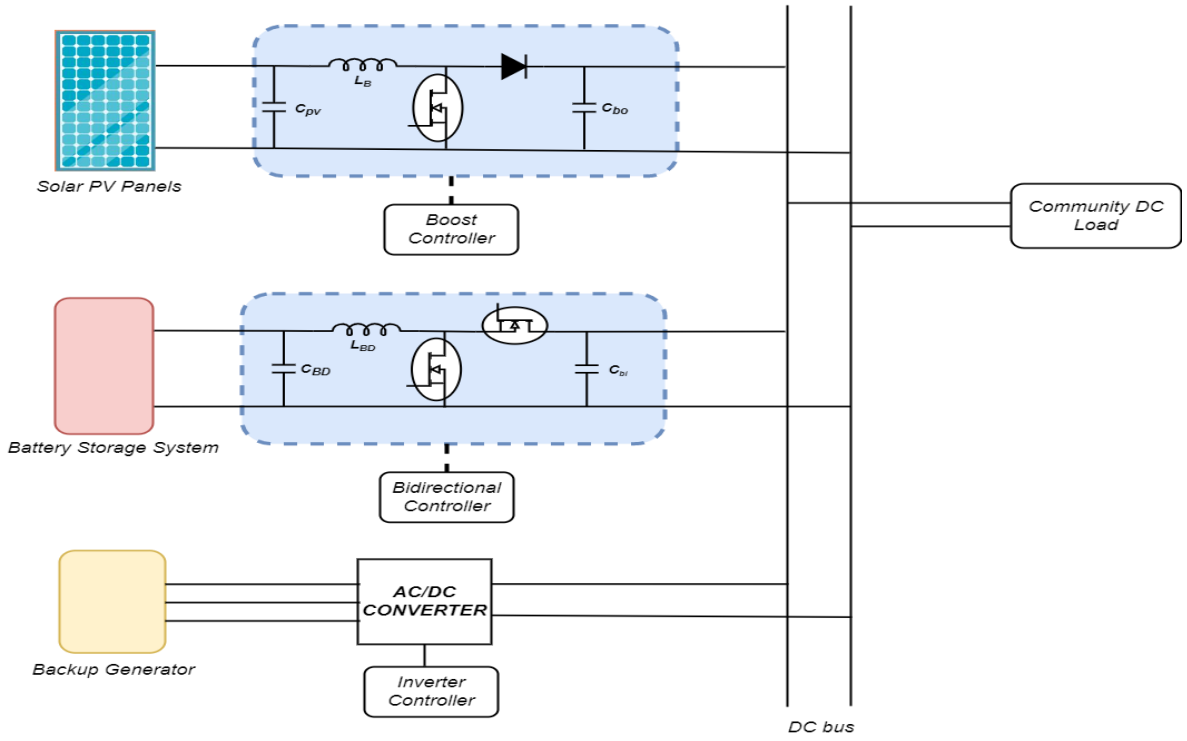

Figure 4 Block Diagram of the studied DC Microgrid.

Table 3 DC microgrid converter parameters values.

Unit	Component	Value
Bidirectional Converter	Inductor	13.38e-6 H
	Capacitor	38.5e-6 F
Boost Converter	Inductor	7.5e-6 H
	Capacitor	1200e-6 F

The microgrid operates in three modes: photovoltaic (PV) mode, battery mode and generator mode. In the PV mode, the solar PV panels primarily supply the load, and the excess power is used to charge the battery. In this mode, the microgrid bus voltage is maintained by the bidirectional DC/DC converter controlled by the central microgrid controller, and the boost converter tracks the

maximum power point (MPPT) of the PV system. When the power generated by the PV system goes lower than the load requirement, the battery system discharges to supply the load. At some point, if the PV power does not increase and the battery voltage falls below the threshold selected, the diesel generator turns on to supply the load, and at the same time charges the battery to avoid damaging the battery. The system will return to the PV mode when the power produced by the solar PV system is enough to service the load and charge the battery back above the desired threshold.

Figure 5 shows the communication topology of the DC microgrid. It can be observed that each converter has a local controller. The local controller sends and receives data from the microgrid central controller (MGCC) to coordinate their operations towards achieving system stability and optimum performance. In this study, the local controllers communicate with the central microgrid controller using the LoRa communication protocol. This is because this study is focused on analyzing the effect of employing LoRa communication for data transfer on microgrid performance.

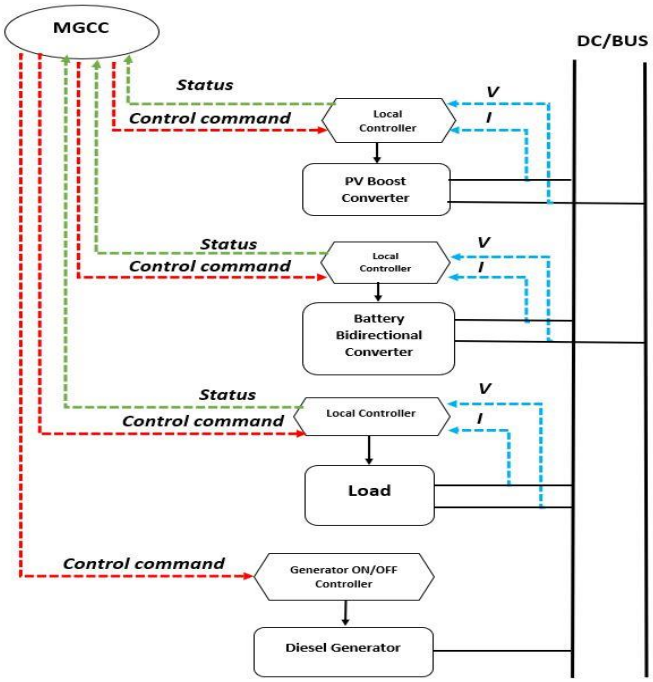

Figure 5 Communication topology of DC microgrid.

The DC microgrid in the paper is controlled using the hierarchical, centralized control method, which is composed of the primary and secondary layers. In the primary layer, there is continuous communication between the sensors and the local controllers monitoring various parameters such as the input/output voltages and/or currents of the various converter depending on the control type as set by the MGCC. Furthermore, in the secondary control, the MGCC assigns the modes of operation depending on the parameter values received from the local controllers to maintain a reliable microgrid operation during the transition between the operation modes. A control logic is implemented within the microgrid central controller for the adopted control scheme to maintain a reliable and optimum operation.

In this study, the DC microgrid was simulated in Matlab/Simulink™ to observe the dynamic performance when the calculated LoRa transmission delays were introduced. The LoRa transmission delay as calculated for the data sent and received is introduced into the communication between

the bidirectional local controller and the MGCC. The effects on the dynamic performance of the microgrid are analyzed during the transition between various modes. These periods are taken into consideration as they are the main events that will trigger required control actions. The DC microgrid was simulated for a period of 4 seconds on Simulink. The switching from the PV mode to the battery mode occurs at t = 1 s, while the switching to the generator mode takes place whenever the battery voltage drops below the threshold and back to the PV mode at t = 3 s. The simulation is then completed at t = 4 s.

The MGCC maintains a normal operation while the load power is being supplied by the solar PV system to service the community load and as well charge the energy storage system. The microgrid DC bus voltage is maintained at 360 V by the DC/DC bidirectional converter controller while the boost converter is MPPT-controlled. When there is a discrepancy between the load power requirement and the power generated by the PV system, the load controller sends a signal (111) to the MGCC. The MGCC then transmits a control signal (000) to the bidirectional converter to switch from the charging mode to the discharging mode to supply the load power requirements. At this period, the DC bus voltage remains controlled by the DC/DC bidirectional converter controller and the battery voltage monitored. when the battery voltage drops below 322.6 V, which corresponds to 50% State of Charge (SOC), to avoid over-discharging of the battery, the MGCC transmits a signal (101) to switch ON the diesel generator to supply the load and at the same time charge the battery system. The diesel generator continues to run until normal conditions such as higher irradiance are restored and MGCC sends a signal (010) to turn OFF the diesel generator and return to the PV operational mode. This microgrid control scheme is shown in Figure 6.

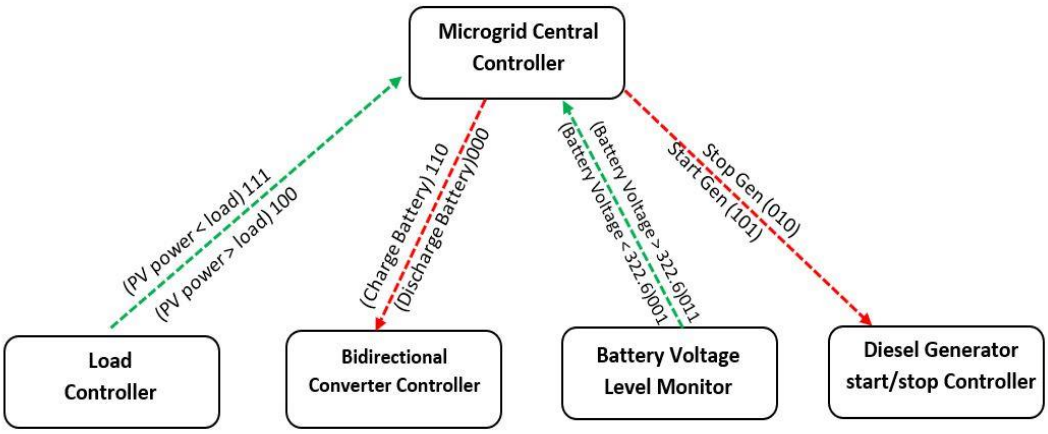

Figure 6 Microgrid control scheme.

5. Simulation Results

This section presents the simulation of the DC microgrid illustrating the switching into the various modes. This shows a normal system without transmission delays, as well as the impact of LoRa transmission delay on the DC bus voltage (V_{DC}), and the voltage across the DC/DC bidirectional converter switch. A transmission delay factor for the signals between the bidirectional local controller and the MGCC was calculated using the Equations (7)-(13) and introduced during communication between the local controllers and the MGCC for transition between the modes after the system control logic decisions have been made at the MGCC.

5.1 Microgrid Normal Operation (No Transmission Delay)

Figure 7 shows the microgrid DC bus voltage during transitions between the modes without communication delays.

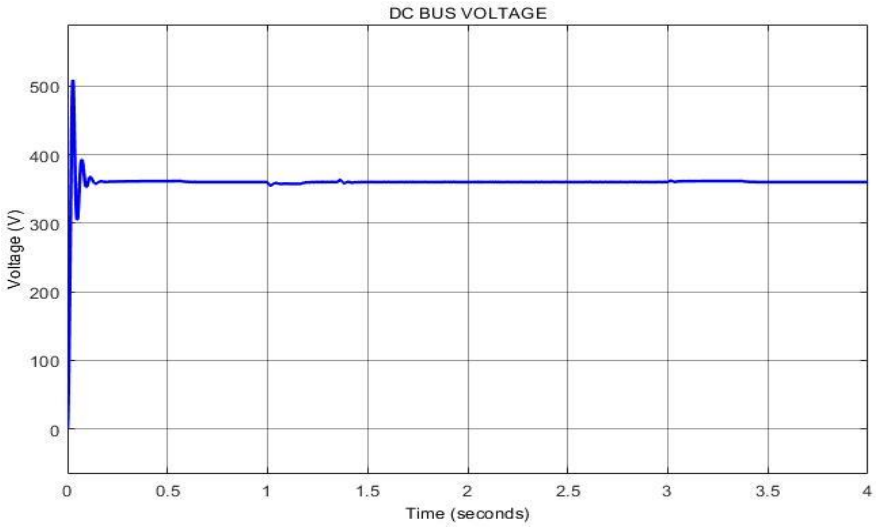

Figure 7 Microgrid DC voltage for simulation without LoRa delay.

Figure 7 shows the DC bus voltage during the simulation time. The figure depicts the stability of the DC bus voltage during the transmission times between the operation modes. The DC bus voltage was maintained at 360 V throughout the simulation time. The voltages of the bidirectional converter with no delays are as shown in Figure 8.

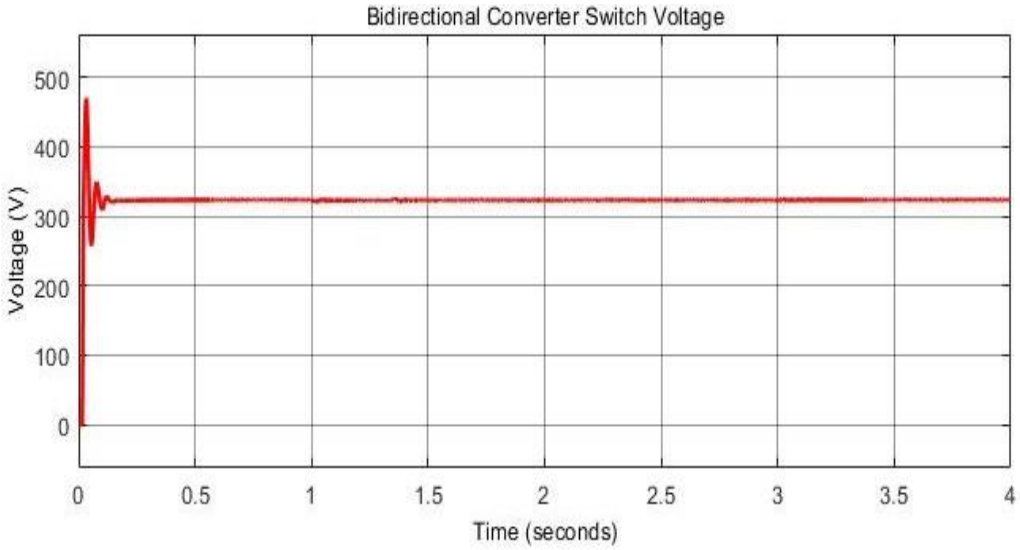

Figure 8 Bidirectional converter switch voltage.

During the operation of the DC microgrid, the battery was also being charged and discharged. Figure 9 shows the charging and discharging process of the energy storage system.

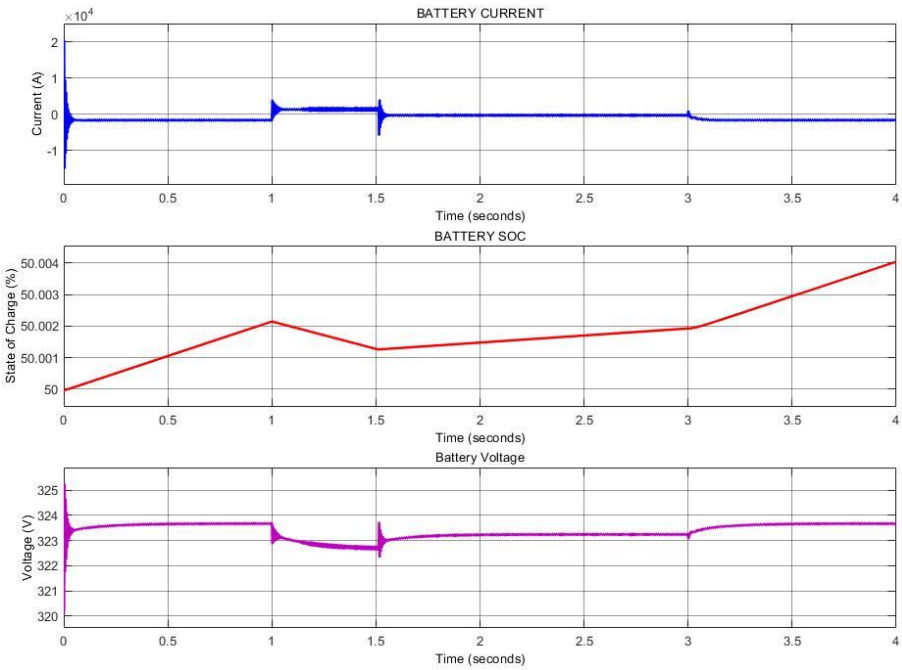

Figure 9 DC microgrid battery parameters.

All the key parameters in Figure 7, Figure 8, Figure 9 show that the system operated at optimum stability across the transition points. This is due to the absence of communication delay in the transmission of measured data and the required control command between the local controllers and the microgrid central controller.

5.2 Microgrid Operation with LoRa Data Transmission Delay

In the studied microgrid, LoRa was employed to send data from the local controllers of the distributed energy resources to the microgrid central controller, and for control commands from the central controller to the local controllers. Therefore, the LoRa transmission delays for transferring each signal between the local controllers and the microgrid central controller using the LoRa communication system were calculated using Equations (7)-(13) and shown in Table 4. For this research, the data was transferred using the highest LoRa bandwidth of 500 KHz. This is because in LoRa transmission, the higher the transmission bandwidth, the lower the transmission delay, as observed from Table 1.

Table 4 Signal Transmission Time.

Signal	Base64 Format	Transmission time (milliseconds)
100	MTAw	10.88
110	MTEw	10.88
111	MTEx	10.88
000	MDAw	10.88
001	MDAx	10.88
011	MDEx	10.88

Therefore, for a complete control process to stabilize the system during the mode switching, a bidirectional data transfer must occur between the local controller and the MGCC. This means two signals must be transmitted. The delay of each signal during the transfer is added, and a total transmission delay of 21.76 ms was calculated and introduced into the system simulation during the mode switching events. The transmission delay was introduced as a transport delay in Simulink representing the data transmission between the local controller of the various microgrid components and the microgrid central controller and vice versa. In this study, the controller computational and processing time are neglected as the focus is on the data transmission time of LoRa communication during data transfer between the MGCC and the local controllers. Figure 10 and Figure 11 show the effect of this transmission delay on the system performance.

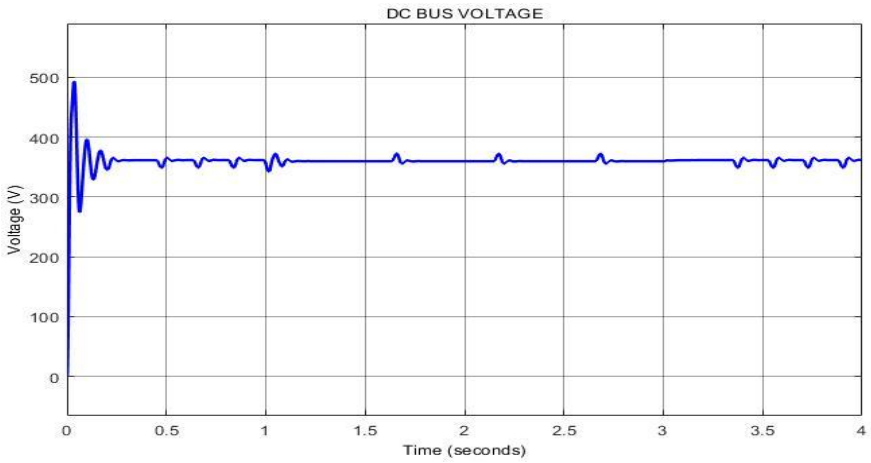

Figure 10 Microgrid DC voltage for simulation with LoRa transmission delay.

Figure 11 Bidirectional converter switch voltage with delay.

From Figure 10, the DC bus voltage shows variations at various points in the simulation time. The transmission delay increased the error between the reference voltage and the measured DC voltage at various instances. At the simulation time 1.19 seconds, the DC voltage spiked to 372.4 V which represents a 4% spike when the power source was switched from the PV source to the battery. We also observed voltage variations at 1.75 s, 2.27 s 2.82 s. furthermore, the DC bus voltage took a negative variation of about 3.8% at 3.325 s, 3.69 s and 3.880 s. This represents a system with a high

level of instability. This instability results from the applied LoRa transmission delays imposed on variations DC bus voltage. Figure 11 also showed the bidirectional converter switch voltage which also has a very large amount of voltage variations caused by the introduction of the LoRa communication delay.

5.3 Mitigating the Effect of LoRa Transmission Delay on DC Bus Voltage

To eliminate the effect of delay on the DC microgrid stability, two system modification scenarios were considered.

5.3.1 Bidirectional Converter LC Component Recalculation

In this method, the DC microgrid bidirectional converter's LC components were re-calculated with consideration of the LoRa communication delay. To compensate for the variation in the bus voltage caused by the communication delay, the converter capacitor value was increased. This capacitor modification had a smoothening effect on the DC bus voltage. The new values of the components are shown in Table 5. The DC bus voltage and the bidirectional converter switch voltage obtained from the redesigned system's simulation are shown in Figure 12 and Figure 13.

Table 5 Signal Transmission Time.

Unit	Component	Value
Bidirectional Converter	Inductor	13.38e-6 H
	Capacitor	45.8e-6 F
Boost Converter	Inductor	7.5e-6 H
	Capacitor	1200e-6 F

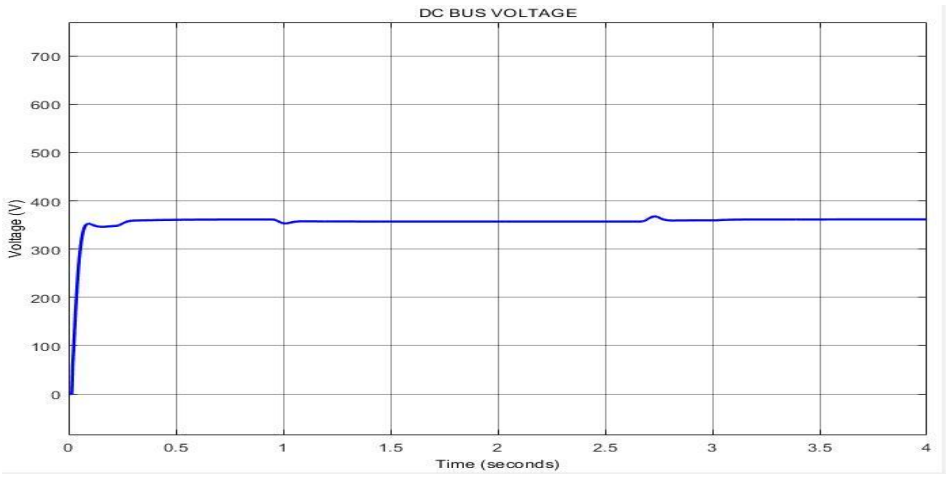

Figure 12 DC bus voltage for redesigned microgrid with LoRa transmission delay.

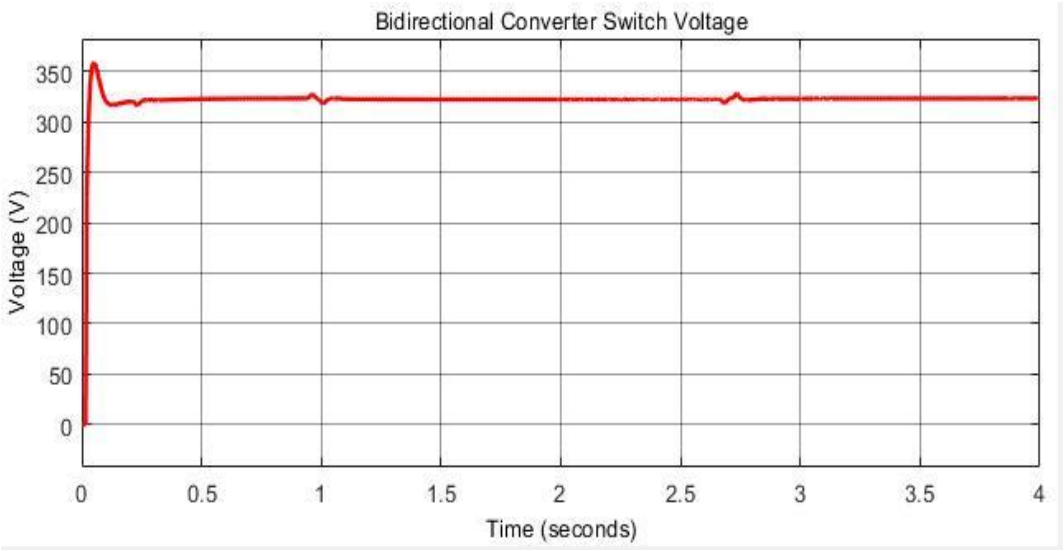

Figure 13 Bidirectional converter switch voltage with modified parameters.

From Figure 12 and Figure 13, a more stable system is observed. The DC bus voltage presented in Figure 12 shows a voltage without much variations, which is almost similar to the DC bus voltage in Figure 7. The voltage in Figure 12 has variations of less than 1% at 1 s and 2.75 s of the simulation. These spikes are relatively small resulting from transitions from the PV mode to the generator mode. However, at 3 s when the microgrid returns to the PV mode due to increase in irradiation, there are no noticeable spikes in the DC bus voltage. Figure 13 shows the bidirectional converter's switch voltage, which also follows the same pattern as the DC bus voltage with slight variations at the same simulations times as with the DC bus voltage.

5.3.2 Modification of the PI Controller for Better System Robustness

In DC microgrids, PI controllers have been used to address time delay effects such as DC bus voltage variations [21-24]. This method involves re-designing the PI controller parameters towards achieving a robust controller system that can maintain system stability even in various system degradation scenarios. After thorough investigation of the controller systems proposed in the literatures, the controller proposed in [24] was applied to the simulation. The proposed system employs a fuzzy-PI dual-mode controller for DC voltage regulation. This controller features speedy response, low overshoot, good robustness, and strong anti-interference under different working conditions allowing for DC voltage stability even with larger transmission delays when compared to results from the controllers proposed in the other literatures. The details on the design and simulation of the proposed technique are fully explained in the literature [24], and as such, not repeated in this paper. The schematic of the employed controller modification is shown in Figure 14. The DC bus voltage obtained from the simulation employing the new controller is shown in Figure 15.

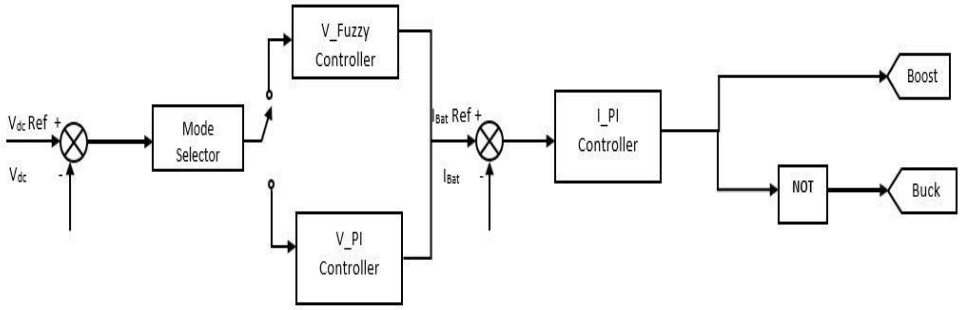

Figure 14 Schematic of modified PI controller in MGCC.

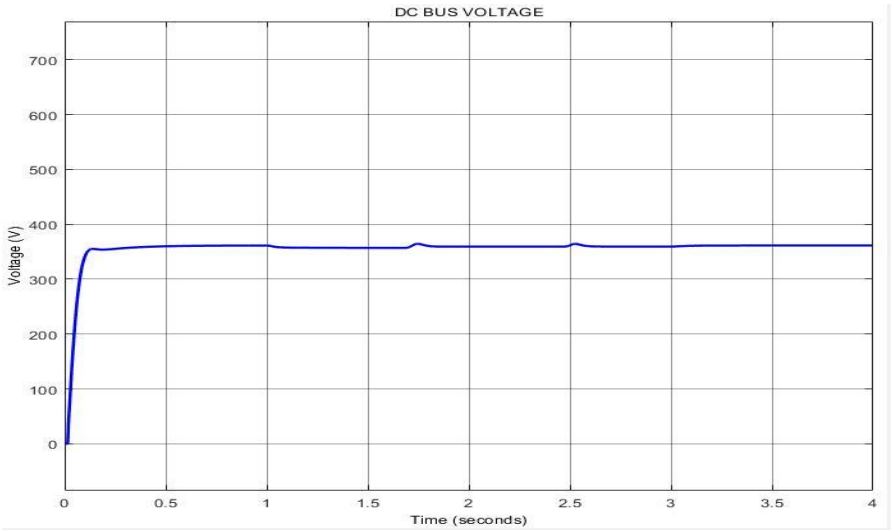

Figure 15 DC microgrid DC bus voltage with modified controller.

The DC bus voltage shown in Figure 15 presents a microgrid with a stable bus voltage even with the introduction of the LoRa communication system. The presented graph shows the presence of very small amount of voltage variations at 1.75 s representing system transition from battery to backup generator supply. There were no voltage variations at 1 s when transitioning from the PV system to the battery supply. Furthermore, another negligible voltage variation was observed at 2.5 s. these variations are minimal and demonstrate that the system still maintains a high level of stability even with the communication delay.

6. Discussion

The first simulation scenario involved a DC microgrid without communication delay. Various key system parameters observed in the results showed that the system operated in optimum stability. However, the introduction of LoRa transmission delay caused reduced system stability demonstrated by spikes in parameters especially while transitioning between various modes. This therefore entails that a stable DC microgrid with the LoRa transmission delay must be achieved. The DC microgrid was therefore simulated for a third scenario. The third simulation was carried out in two scenarios.

In the first simulation, only the LC components of the bidirectional converter were re-calculated and re-designed. The new component values were employed, and the system was re-simulated. The

results obtained showed that the delay imposed on the system by LoRa was not large, and a simple re-calculation of the system parameters achieved a more stable performance.

In the second stability test, the PI controller was modified with additional functionalities to improve the robustness of the system in Matlab/Simulink™. The results also showed a DC voltage with reduced spikes. The PI controller modifications allowed for system stability even for a larger delay time.

The results obtained from the simulations in the delay mitigation section exhibit a stable system even during the transitions with the delays incorporated. This therefore confirms that with a refined system design, LoRa communication can be employed for data transfer and still achieve system stability.

Furthermore, the results also showed that the communication system to be employed for data transfer within a microgrid should be put into consideration in the microgrid design stages especially if low bandwidth communication is to be employed.

7. Conclusions and Future Work

In this paper, the effects of LoRa transmission delay on the dynamic performance of a DC microgrid was analyzed. This analysis was carried out to observe how the microgrid would function when a low bandwidth communication system such as LoRa is employed for data transfer at the secondary control level. For a centralized communication-based controlled microgrid as presented in the paper, a very reliable communication structure is required. Data transmission delay is therefore a very important factor towards achieving a stable microgrid operation. To complete the analysis, a DC microgrid was simulated in Matlab/Simulink™. The microgrid operated in three modes: namely, PV mode, battery mode and generator mode. The system was simulated for three scenarios to understand system function without transmission delay, with LoRa transmission delay and with the system parameters re-calculated and re-designed to achieve stability. Our analysis and simulations indicate that LoRa transmission delay can be compensated for within the systems controllers.

As a recommendation for future work, ways of extending LoRa communication range for its application to large area microgrids will be very important. This is because, microgrids have DERs at various distances, and the distance of LoRa coverage generally has a negative effect on the transmission delay. This will, in turn have a negative effect on microgrid stability.

Acknowledgments

The authors would like to thank the School of Graduate Studies, Faculty of Engineering and Applied Science, Memorial University of Newfoundland for providing a conducive environment to carry out this research.

Author Contributions

Cherechi Ndukwe: Carried out the design and simulations and wrote the manuscript. M. Tariq Iqbal, Jahangir Khan and Mohsin Jamil supervised the project and contributed to the final version of the manuscript.

Competing Interests

The authors have declared that no competing interests exist.

References

1. Saleh MS, Althaibani A, Esa Y, Mhandi Y, Mohamed AA. Impact of clustering microgrids on their stability and resilience during blackouts. Proceedings of 2015 International Conference on Smart Grid Clean Energy Technologies (ICSGCE); 2015 October 20-23; Offenburg, Germany. New York: IEEE.
2. Saleh M, Esa Y, Mhandi Y, Brandauer W, Mohamed A. Design and implementation of CCNY DC microgrid testbed. Proceedings of 2016 IEEE Industry Applications Society Annual Meeting; 2016 October 02-06; Portland, Oregon, USA. New York: IEEE.
3. Ton DT, Smith MA. The US department of energy's microgrid initiative. Electr J. 2012; 25: 8.
4. Hatziargyriou N. Microgrids: Architectures and control. New York: John Wiley & Sons; 2013. pp. 4-70.
5. Saleh M, Esa Y, Mohamed AA. Communication-based control for DC microgrids. IEEE Trans Smart Grid. 2019; 10: 2180-2195.
6. Hossain E, Kabalci E, Bayindir R, Perez R. Microgrid testbeds around the world: State of art. Energy Convers Manag. 2014; 86: 132-153.
7. Liu Z, Xu X, Abdelsalam HA, Makram E. Power system harmonics study for unbalanced microgrid system with PV sources and nonlinear loads. J Power Energy Eng. 2015; 3: 43-55.
8. Backhaus SN, Swift GW, Chatzivasileiadis S, Tschudi W, Glover S, Starke M, et al. DC scoping study. Estimate of technical and economic benefit. Los Alamos National Lab. (LANL), Los Alamos, NM (United States); 2015; LA-UR-15-22097.
9. Chen D, Xu L. Autonomous DC voltage control of a DC microgrid with multiple slack terminals IEEE Trans. Power Syst. 2012; 27: 1897-1905.
10. Balog RS. Autonomous local control in distributed DC power systems. Urbana-Champaign: University of Illinois at Urbana-Champaign; 2006.
11. Ito Y, Zhongqing Y, Akagi H. DC microgrid based distribution power generation system. Proceedings of the 4th International Power Electronics and Motion Control Conference; 2004 August 14-16; Xi'an, China. New York: IEEE.
12. Lee JH, Kim HJ, Han BM. Operation analysis of a communication-based DC micro-grid using a hardware simulator. J Power Electron. 2013; 13: 313-321.
13. Pinomaa A, Ahola J, Kosonen A. Power-line communication-based network architecture for LVDC distribution system. Proceedings of 2011 IEEE International Symposium on Power Line Communications and Its Applications; 2011 April 03-06; Udine, Italy. New York: IEEE.
14. Ndukwe C, Iqbal T, Liang X, Khan J, Aghenta LO. LoRa-based communication system for data transfer in microgrids. AIMS Electron Electr Eng. 2020; 4: 303-325.
15. Zhao J, Dörfler F. Distributed control and optimization in DC microgrids. Automatica. 2015; 61: 18-26.
16. Khorsandi A, Ashourloo M, Mokhtari H. A decentralized control method for a low-voltage DC microgrid. IEEE Trans Energy Convers. 2014; 29: 793-801.
17. Heemels WPMH, Sandee JH, Van den Bosch PPJ. Analysis of event-driven controllers for linear systems. Int J Control. 2008; 81: 71-590.

18. Sandee JH, Heemels WPMH, Van den Bosch PPJ. Case studies in event-driven control. Proceedings of the 10th International Workshop on Hybrid Systems: Computation and Control (HSCC 2007); 2007 April 03-05; Pisa, Italy. Berlin, Heidelberg: Springer.
19. Lu X, Guerrero JM, Sun K, Vasquez JC. An improved droop control method for DC microgrids based on low bandwidth communication with DC bus voltage restoration and enhanced current sharing accuracy. IEEE Trans Power Electron. 2014; 29: 1800-1812.
20. Haritsa TR, Yashu B, Kumar UV, Suma MN. Mathematical characterization and simulation of LoRa. Wirel Pers Commun. 2020; 115: 1481-1506.
21. Zhang W, Fang Y, Ye R, Wang Z. Analysis and design of a double fuzzy PI controller of a voltage outer loop in a reversible three-phase PWM converter. Energies. 2020; 13: 3778.
22. Elnady A. PI controller based operational scheme to stabilize voltage in microgrid. Proceedings of the 2019 Advances in Science and Engineering Technology International Conferences (ASET); 2019 March 26-April 10; Dubai, United Arab Emirates. New York: IEEE.
23. Barbosa RA, De Almeida Souza D, Da Nóbrega Tahim AP. Adaptive control of DC microgrid using PI controller and fuzzy inference. Proceedings of 2019 IEEE PES Innovative Smart Grid Technologies Conference - Latin America (ISGT Latin America); 2019 September 15-18; Gramado, Brazil. New York: IEEE.
24. Zhang Y, Wei S, Wang J, Zhang L. Bus voltage stabilization control of photovoltaic DC microgrid based on fuzzy-PI dual-mode controller. J Electr Comput Eng. 2020; 2020: 2683052.